

# Theoretical study of $\text{HfF}^+$ for the electron EDM search

A.N. Petrov,<sup>1,\*</sup> N.S. Mosyagin,<sup>1</sup> and A.V. Titov<sup>1,†</sup>

<sup>1</sup>*Petersburg Nuclear Physics Institute, Gatchina, Leningrad district 188300, Russia*

We report *ab initio* relativistic correlation calculations of potential curves and electric dipole transition moments for ten low-lying electronic states, effective electric field on the electron, hyperfine constants and radiative lifetimes for the  $^3\Delta_1$  state of cation of the heavy transition metal fluoride  $\text{HfF}^+$ , which it is suggested to be used in experiments to search for the electric dipole moment of the electron. It is obtained that  $\text{HfF}^+$  has deeply bound  $^1\Sigma^+$  ground state; its dissociation energy is  $D_e = 6.4$  eV. The  $^3\Delta_1$  state is obtained as the relatively long-lived, with lifetime equal to about 0.4 s., first excited state lying about 0.2 eV higher. The calculated effective electric field,  $E_{\text{eff}} = W_d|\Omega|$ , acting on an electron in this state is  $5.84 \times 10^{24} \text{ Hz}/e$  cm. The obtained hyperfine constants are  $A_{\parallel} = -1239$  MHz for the  $^{177}\text{Hf}$  nucleus and  $A_{\parallel} = -58.1$  MHz for the  $^{19}\text{F}$  nucleus.

## INTRODUCTION.

The search for the electric dipole moment (EDM) of the electron ( $d_e$  or eEDM below) remains one of the most fundamental problems in physics. Up to now only upper limits for  $|d_e|$  were obtained. The tightest bound on  $d_e$  was given in the experiment on the atomic Tl beam [1], which established an upper bound of  $|d_e| < 1.6 \times 10^{-27} e$  cm ( $e$  is the charge of the electron). Molecular systems provide a way to get much enhanced sensitivity, since the effective intramolecular electric field acting on electrons in polar molecules can be five or more orders of magnitude higher than the strongest field available in the laboratory [2, 3, 4].

The new generation of the eEDM experiments, employing polar heavy-atom molecules, is expected to reach sensitivity of  $10^{-30}$ – $10^{-28} e$  cm/ $\sqrt{\text{day}}$  (e.g., see [5]). Their results are expected to dramatically influence all the popular extensions of the Standard model, in particular supersymmetry, even if bounds on the  $P, T$ -odd effects compatible with zero are obtained (see [6, 7] and references therein). These studies include the beam experiments carried out on YbF molecular radicals by Hinds and co-workers [5], and the vapor cell experiment on the metastable  $a(1)$  state of PbO prepared by the group of DeMille and co-workers (see [8] and references therein). New ways of searching for the eEDM, using trapped cold molecular cations, were investigated during the last years by Cornell and co-workers. The first candidate was  $\text{HI}^+$  [9], but subsequent estimate [10] and accurate calculation [11] have shown that this cation has rather small  $E_{\text{eff}}$  (see below). Then some other candidates were considered,  $\text{HfH}^+$  [12],  $\text{HfF}^+$  [13] etc., having  $^3\Delta_1$  as the ground or probably long-lived excited state. Even experimental study of spectroscopic properties for these cations is a very difficult problem, and there are no such data measured up to date though they are already required to analyze basic stages of the eEDM experiment [13]. In turn, the modern relativistic computational methods can now give reliable answers to almost all the questions of interest even for compounds of heavy transition metals

as is in our case. In the paper [14] a theoretical study of the required spectroscopic properties,  $E_{\text{eff}}$  and hyperfine structure, of  $\text{HfF}^+$  as a candidate for the eEDM experiment was performed. In particular, it was shown that  $^3\Delta_1$  is not the ground state, its radiative lifetime was estimated as 0.5 sec. In the present paper the above study is discussed in more details and, besides, new obtained data are given. In particular, the more accurate data for the transition dipole moment  $^1\Sigma^+ \rightarrow ^3\Delta_1$  and, consequently, more reliable values for the radiative lifetimes of the lowest vibrational levels of the  $^3\Delta_1$  are presented. Also the obtained data for other transition dipole moments can be used to study possible schemes of populating the  $^3\Delta_1$  state. With using the Dirac-Hartree-Fock calculations it was suggested in [14] that influence of  $4f$  electrons of Hf is negligible for the excitation energy  $^1\Sigma^+ \rightarrow ^3\Delta_1$ . Taking into account the importance of this conclusion for the accuracy analysis, in the present paper the influence of correlation of the  $4f$  electrons is studied here.

## $E_{\text{eff}}$ AND HYPERFINE STRUCTURE.

One of the most important features of such experiments is that knowledge of the effective electric field  $E_{\text{eff}}$  seen by an unpaired electron is required for extracting  $d_e$  from the measurements.  $E_{\text{eff}}$  cannot be obtained in an experiment; rather, electronic structure calculations are required for its evaluation. It is given by the expression  $E_{\text{eff}} = W_d|\Omega|$ , where  $W_d$  is a parameter of the  $P, T$ -odd molecular Hamiltonian that is presented in Refs. [4, 15, 16],

$$W_d = \frac{1}{\Omega d_e} \langle \Psi | \sum_i H_d(i) | \Psi \rangle, \quad (1)$$

where  $\Psi$  is the wave function for the  $^3\Delta_1$  state, and  $\Omega = \langle \Psi | \mathbf{J} \cdot \mathbf{n} | \Psi \rangle = \pm 1$ ,  $\mathbf{J}$  is the total electronic momentum,  $\mathbf{n}$  is the unit vector along the molecular axis directed from Hf to F,

$$H_d = 2d_e \begin{pmatrix} 0 & 0 \\ 0 & \boldsymbol{\sigma} \mathbf{E} \end{pmatrix}, \quad (2)$$

$\mathbf{E}$  is the inner molecular electric field, and  $\boldsymbol{\sigma}$  are the Pauli matrices. The  $E_{\text{eff}}$  value for the  ${}^3\Delta_1$  state was estimated in the scalar-relativistic approximation by Meyer *et al.* (see the note added at the end of [17]) and the method used for calculation of  $E_{\text{eff}}$  is close in essence to that developed by Titov earlier [18] and applied to two-step calculations of the PbF molecule [15, 18]. In paper [14] a more reliable value of  $E_{\text{eff}}$  is calculated using the advanced two-step technique developed by Titov and co-workers later [19, 20, 21, 22]. The hyperfine constants for  ${}^{177}\text{Hf}$  and  ${}^{19}\text{F}$  nuclei ( $A_{\parallel}[\text{Hf}]$  and  $A_{\parallel}[\text{F}]$ ) for the  ${}^3\Delta_1$  state of  $\text{HfF}^+$  are also calculated. The hyperfine constants are determined by expression [23]

$$A_{\parallel}[\text{Hf}(\text{F})] = \frac{1}{\Omega} \frac{\mu_{\text{Hf}(\text{F})}}{I_{\text{Hf}(\text{F})}} \langle \Psi | \sum_i \left( \frac{\boldsymbol{\alpha}_i \times \mathbf{r}_i}{r_i^3} \right)_Z | \Psi \rangle, \quad (3)$$

where  $I_{\text{Hf}(\text{F})}$  and  $\mu_{\text{Hf}(\text{F})}$  are the spin momentum and magnetic moment of  ${}^{177}\text{Hf}({}^{19}\text{F})$ ,  $\boldsymbol{\alpha}_i$  are the Dirac matrices for the  $i$ -th electron, and  $\mathbf{r}_i$  is its radius-vector in the molecular coordinate system centered on the Hf or F atom. When the experimental value  $A_{\parallel}[\text{Hf}]$  is measured, it provides an accuracy check for the calculated  $E_{\text{eff}}$  value. Both  $A_{\parallel}[\text{Hf}]$  and  $A_{\parallel}[\text{F}]$  values are useful for identifying  $\text{HfF}^+$  by its spectrum from other species in the experiment.

## METHODS AND CALCULATIONS

### The GRECP method.

When core electrons of a heavy-atom molecule do not play an active role (i.e., their relaxation in the molecule is negligible) the effective Hamiltonian with relativistic effective core potential (RECP) can be presented in the form

$$\mathbf{H}^{\text{Ef}} = \sum_{i_v} \left[ \mathbf{h}^{\text{Schr}}(i_v) + \mathbf{U}^{\text{Ef}}(i_v) \right] + \sum_{i_v > j_v} \frac{1}{r_{i_v j_v}}. \quad (4)$$

Hamiltonian (4) is written only for a valence subspace of electrons, which are treated explicitly and denoted by indices  $i_v$  and  $j_v$ . In practice, this subspace is often extended by inclusion of some outer core shells for better accuracy. In Eq. (4),  $\mathbf{h}^{\text{Schr}}$  is the one-electron Schrödinger Hamiltonian

$$\mathbf{h}^{\text{Schr}} = -\frac{1}{2} \nabla^2 - \frac{Z_{ic}}{r}, \quad (5)$$

where  $Z_{ic}$  is the charge of the nucleus decreased by the number of inner core electrons.  $\mathbf{U}^{\text{Ef}}$  is an RECP (or relativistic pseudopotential (PP)) operator that can be written in the separable (e.g., see Ref. [24] and references therein) or radially-local (semi-local)[25] approximations when the valence pseudospinors are smoothed in heavy-atom cores. This smoothing allows one to reduce the number of primitive Gaussian basis functions required for appropriate description of valence spinors in subsequent molecular calculations and also to exclude the small components of the four-component Dirac spinors from the RECP calculations, with relativistic effects being taken into account by  $j$ -dependent effective potentials. Contrary to the four-component wave function used in Dirac-Coulomb(-Breit) calculations, the pseudo-wave function in the RECP case can be both two- and one-component.

Besides, the generalized RECP (GRECP) operator[26, 27] can be used in Eq. (4) that includes the radially-local, separable and Huzinaga-type[28] relativistic PPs as its components and some special cases. The GRECP concept was introduced and developed in a series of papers (see Refs. [26, 27, 29, 30, 31, 32] and references therein). In contrast to other RECP methods, GRECP employs the idea of separating the space around a heavy atom into three regions: inner core, outer core and valence, which are treated differently. It allows one to attain theoretically any desired accuracy, while requiring moderate computational efforts since the overall accuracy is limited in practice by possibilities of correlation methods.

Two of the major features of the GRECP version with the separable correction described here are generating of the effective potential components for the pseudospinors which may have nodes, and addition of non-local separable terms with projectors on the outer core pseudospinors to the conventional semi-local RECP operator. The problem of division by zero appearing in the cases of pseudospinors with nodes is overcome in the GRECP method by interpolating the corresponding potentials in the vicinity of these nodes[33, 34]. It was shown both theoretically and computationally that the interpolation errors are small enough. That allows us to generate different potentials for the cases of outer core and valence pseudospinors with the same quantum numbers  $l$  and  $j$ , unlike the conventional RECP approach. In turn, the non-local separable terms in the GRECP operator account for difference between these potentials, which in the outer region is defined by smoothing within the inner core as is shown in Ref. [35, 36, 37] and in many cases this difference can not be neglected for “chemical accuracy” (about 1 kcal/mol or 350  $\text{cm}^{-1}$ ) of valence energies. The more circumstantial description of distinctive features of the GRECP as compared to the original RECP schemes is given in Refs. [38, 39]. Some other GRECP versions are described and discussed in details in Refs. [26, 27, 31].

The GRECP operator in the spinor representation[26, 40] is naturally used in atomic calculations. The spin-

orbit representation of this operator which can be found in Ref. [26, 41] is more efficient in practice being applied to calculation of molecules. Despite the complexity of expression for the GRECP operator, the calculation of its one-electron integrals is not notably more expensive than that for the case of the conventional radially-local RECP operator.

The GRECP simulating interaction of 12 outercore and valence electrons of Hf with the explicitly excluded 1s to 4f electrons (60 inner core electrons) is used in 20-electron calculations of HfF<sup>+</sup>.

### Freezing the innermost shells from the outer core space.

The “freezing” of innermost shells from the outer core space of electrons within the “small core” GRECPs is sometimes required because the accuracy of the GRECPs generated directly for a given number of explicitly treated electrons cannot always correspond to the accuracy of the conventional “frozen core” approximation with the same space of explicitly treated electrons (without accounting for the frozen states). That space is usually chosen as a minimal one required for attaining a given accuracy. It was noted in Refs. [34, 40] that using essentially different smoothing radii for spinors with different  $lj$  is not expedient since the (G)RECPs errors are mainly accumulated by the outermost from them. In turn, explicit treatment of all of the outer core shells of an atom with the same principal quantum number is not usually reasonable in molecular (G)RECP calculations because of essential increase in computational efforts without serious improvement of accuracy. A natural way out is to “freeze” the innermost of them before performing molecular calculation but this can not be done directly if the spin-orbit molecular basis set is used whereas the core shells should be better frozen as spinors.

In order to exclude (“freeze”) explicitly those innermost shells (denoted by indices  $f$  below) from molecular (G)RECP calculation without changing the radial node structure of other (outermore core and valence) shells in the core region, the energy level shift technique can be applied to overcome the above contradiction [26, 42]. Following Huzinaga *et al.* [28], one should add the effective core operator  $\mathbf{U}_{\text{Huz}}^{\text{Ef}}$  containing the Hartree-Fock field operators, the Coulomb ( $\tilde{\mathbf{J}}$ ) and spin-dependent exchange ( $\tilde{\mathbf{K}}$ ) terms, over these core spinors together with the level shift terms to the one-electron part of the Hamiltonian (4):

$$\mathbf{U}_{\text{Huz}}^{\text{Ef}} = (\tilde{\mathbf{J}} - \tilde{\mathbf{K}})[\tilde{f}_{n_f l_j}] + \sum_{n_f, l, j} B_{n_f l_j} |\tilde{f}_{n_f l_j}\rangle\langle\tilde{f}_{n_f l_j}| \quad (6)$$

$$\text{(i.e. } \varepsilon_{n_f l_j} \rightarrow \varepsilon_{n_f l_j} + B_{n_f l_j} \text{)},$$

where  $|\tilde{f}_{n_f l_j}\rangle\langle\tilde{f}_{n_f l_j}|$  are the projectors on the core spinors  $\tilde{f}_{n_f l_j}$  and  $\varepsilon_{n_f l_j}$  are their one-electron energies. The  $B_{n_f l_j}$  parameters are presented as  $M|\varepsilon_{n_f l_j}|$  in our codes and  $M > 1$  to prevent occupying the corresponding states in calculations; it is usually selected as  $M \gg 1$  in our studies. Such nonlocal terms are needed in order to prevent collapse of the valence electrons to the frozen core states. They introduce some “soft orthogonality constraint” between the “frozen” and other explicitly treated outermore core and valence electronic states.

All the terms with the frozen core spinors (the level shift operator and exchange interactions) can be transformed to the spin-orbit representation in addition to the spin-independent Coulomb term, using the identities for the  $\mathbf{P}_{lj}$  projectors[43]:

$$\mathbf{P}_{l, j=l\pm 1/2} = \frac{1}{2l+1} \left[ \left( l + \frac{1}{2} \pm \frac{1}{2} \right) \mathbf{P}_l \pm 2\mathbf{P}_l \vec{\mathbf{l}} \cdot \vec{\mathbf{s}} \mathbf{P}_l \right], \quad (7)$$

$$\mathbf{P}_{lj} = \sum_{m_j=-j}^j |ljm_j\rangle\langle lj m_j|,$$

$$\mathbf{P}_l = \sum_{m_l=-l}^l |lm_l\rangle\langle lm_l|.$$

where  $\vec{\mathbf{l}}$  and  $\vec{\mathbf{s}}$  are operators of the orbital and spin momenta,  $|ljm_j\rangle\langle lj m_j|$  is the projector on the two-component spin-angular function  $\chi_{ljm_j}$ ,  $|lm_l\rangle\langle lm_l|$  is the projector on the spherical function  $Y_{lm_l}$ .

More importantly, these outer core pseudospinors can be frozen in calculations with the *spin-orbit* basis sets and they can already be frozen at the stage of calculation of the one-electron matrix elements of the Hamiltonian, as implemented in the MOLGEP code [44]. Thus, any integrals with indices of the frozen spinors are completely excluded after the integral calculation step. The multiplier  $M=30$  was chosen in the present molecular calculations to prevent mixing the shifted core states to the wavefunction due to correlations but not to get poor reference wavefunction in the initial spin-averaged calculations at the same time (as would be for  $M \rightarrow \infty$ ).

In fact, the *combined* GRECP version, with separable and Huzinaga-type terms, is a new pseudopotential treating some minimal number of electrons explicitly but which already provide the accuracy approaching to that of the frozen core approximation. The efficiency of using the “freezing” procedure within the GRECP method was first studied in calculations of Tl [26] and TIH [42].

In ten-electron calculations, which are substantially less time consuming, 5s and 5p spinors of hafnium and 1s orbital of fluorine are frozen from the states averaged over the nonrelativistic configurations  $5d^26s^{0.6}6p^{0.4}$  for Hf<sup>+</sup> and  $2s^22p^5$  for F, and not treated explicitly.

### The SODCI method.

The spin-orbit direct configuration interaction (SODCI) method is well described in papers [45, 46]. In the current version of the method, calculations are carried out in the  $\Lambda S$  basis set of many-electron spin-adapted (and space symmetry-adapted) functions (SAFs). The different  $\Lambda S$  sets of SAFs are collected together in accord to the relativistic double-group symmetry requirements for the final configuration interaction (CI) calculation. In the present study of the molecule having the  $2S'+1A'$  leading term, configurations from all the symmetry allowed  $\Lambda S$  sets with  $S \leq 2$  are included into calculations.

All the possible singly and doubly excited configurations with respect to some reference configurations are generated (see below for choice of the reference configurations). A generated configuration is included in the final CI space if its addition to the reference set leads to lowering in the total energy by the value more than some threshold  $T$ . This lowering is estimated with the help of the  $A_k$  version of perturbation theory [47], in which the correlation and spin-orbit interaction are considered as perturbations and the wavefunction (obtained from the CI calculation in the space of the reference configurations for all the  $\Lambda S$  irreducible representations) is taken as a zero approximation (see [22, 42] for details). The lowerings in the total energies for the unselected configurations are employed for the  $T=0$  threshold extrapolation. The generalized multireference analogue [48] of the Davidson correction [49] (full CI correction) is also calculated.

In the present calculations, those configurations are chosen as the reference (main) configurations which give the largest contribution to the wavefunction (i.e. have the largest square of the absolute value of the CI coefficient ( $C_I$ ), and thus, that  $C_{ref}^2 \equiv \sum_{I \in \text{ref}} |C_I|^2 = C$ , where  $C = 0.973$  for ten-electron and  $C = 0.942$  for 20-electron calculations. The configurations are obtained from results of the preliminary SODCI calculations in the relativistic double-group symmetry with the large threshold  $T$ . New SODCI calculation is then carried out with the smaller thresholds. The  $C$  is taken the same for each point on the potential curve [50]. Davidson and other corrections estimating contributions for higher than double excitations have an essential dependence on  $C_{ref}^2$ . The above selection criterion allows one to stabilize these corrections for different internuclear distances. This is important because the reliability of those corrections has a significant dependence on these values.

### Basis sets and property calculations.

The generalized correlation atomic basis set [51, 52] ( $12s16p16d10f10g$ )/( $6s5p5d3f1g$ ) is constructed for Hf. The ANO-L ( $14s9p4d3f$ )/( $4s3p2d1f$ ) atomic basis set

listed in the MOLCAS 4.1 library [53] was used for fluorine. The molecular orbitals are obtained by the complete active space self-consistent field (CASSCF) method [53, 54] with the spin-averaged part of the GRECP [26], i.e. only scalar-relativistic effects are taken into account at this stage. In the CASSCF method, orbitals are subdivided into three groups: inactive, active, and virtual. Inactive orbitals are doubly occupied in all the configurations; all possible occupations are allowed for active orbitals, whereas virtual orbitals are not occupied. So the wave function is constructed as a full configuration-interaction expansion in the space of active orbitals, and both active and inactive orbitals are optimized for subsequent correlation calculations of  $\text{HfF}^+$ . According to the  $C_{2v}$  point group classification scheme used in our codes, five orbitals in  $A_1$ , four in  $B_1$  and  $B_2$ , and two in  $A_2$  irreducible representations (irreps) are included in the active space. In ten-electron calculations, one orbital in the  $A_1$  irrep (which is mainly the  $2s$  orbital of F) belongs to the inactive space. In 20-electron CASSCF calculations, the  $5s$  and  $5p$  orbitals of Hf and  $1s$  orbital of F are added to the space of inactive orbitals.

The ten lowest states with the leading configurations  $[...] \sigma_1^2 \sigma_2^2$  ( $1\Sigma^+$ ),  $[...] \sigma_1^2 \sigma_2^1 \delta^1$  ( $3\Delta_{1,2,3}$ ;  $1\Delta$ ),  $[...] \sigma_1^2 \sigma_2^1 \pi^1$  ( $3\Pi_{0-,0+,1,2}$ ;  $1\Pi$ ) were calculated. Here the  $\sigma_1$  orbital is mainly formed by the  $2p_z$  orbital of F with admixture of the  $6p_z$  and  $6s$  orbitals of Hf,  $\sigma_2$  is mainly the  $6s$  orbital of Hf with admixture of the  $6p_z$  orbital of Hf,  $\delta$  and  $\pi$  are mainly the  $5d$  orbitals of Hf.

To obtain the spectroscopic parameters, six points listed in table I and a point at 100 a.u. on the  $\text{HfF}^+$  potential curves were calculated for ten lowest-lying states in ten-electron calculations and for four states in 20-electron ones. The 20-electron calculation is substantially more time consuming; therefore the remaining six states were calculated for only one point, 3.4 a.u., in the present study. Comparing the latter calculations with corresponding ten-electron ones, the core ( $5s^2$  and  $5p^6$  shells of Hf and  $1s^2$  shell of F) relaxation and correlation corrections to the  $T_e$  values, called ‘‘core corrections’’ below and in Table III, were estimated. Only the electronic  $1\Sigma^+$  state is below the  $3\Delta_1$  one. The radiative lifetime of the lowest vibrational levels of the latter with respect to its decay to the vibrational levels of the  $1\Sigma^+$  state can be written (here we are neglecting the rotational structure of the considered states) as

$$\tau_{\text{el}(3\Delta_1, v_2)}^{-1} = \frac{4}{3c^3} \sum_{v_1(\Delta E > 0)} \Delta E^3 | \langle \Psi_{3\Delta_1, v_2} | \mathbf{d} | \Psi_{1\Sigma^+, v_1} \rangle |^2, \quad (8)$$

where  $\Delta E = (E_{(3\Delta_1, v_2)} - E_{(1\Sigma^+, v_1)})$  is the difference in the energies of the electronic-vibrational states  $\Psi_{3\Delta_1, v_2}$  and  $\Psi_{1\Sigma^+, v_1}$ ;  $\mathbf{d}$  is the dipole moment operator. In the adiabatic approximation

$$| \langle \Psi_{3\Delta_1, v2} | \mathbf{d} | \Psi_{1\Sigma^+, v1} \rangle |^2 = | \langle \mathcal{X}_{3\Delta_1, v2}(R) | D(R)_{1\Sigma^+ \rightarrow 3\Delta_1} | \mathcal{X}_{1\Sigma^+, v1}(R) \rangle |^2, \quad (9)$$

where  $\mathcal{X}_{3\Delta_1, v2}(R)$  is the vibrational wave function of the given electronic state and  $D(R)_{1\Sigma^+ \rightarrow 3\Delta_1}$  is the electronic transition dipole moment as a function of the internuclear distance. The excited vibrational levels of the  ${}^3\Delta_1$  state can also decay to the lower vibrational levels of the same,  ${}^3\Delta_1$ , electronic state. The radiative lifetime  $\tau_{\text{vibr}}$  of this process is determined by the equations similar to (8) and (9) with replacing  ${}^1\Sigma^+$  by  ${}^3\Delta_1$ .  $D(R)_{3\Delta_1 \rightarrow 3\Delta_1}$  here is the total molecule-frame electric dipole moments for  ${}^3\Delta_1$  state of the cation, calculated with respect to the center of mass. In Table I we tabulated  $D^{10e}(R)$  for six points using the electronic wave functions obtained in the ten-electron calculations. In Table II we listed  $D^{20e}(R)$  for point 3.4 a.u. using the electronic wave functions obtained in the twenty-electron calculations. To calculate the radiative lifetimes in according to eqs. (8) and (9) we first use the  $D^{10e}(R)$  values and then multiply the obtained  $\tau_{\text{el}}$  and  $\tau_{\text{vibr}}$  on the corresponding correction factors  $(D^{10e}(3.4)/D^{20e}(3.4))^2$ . The vibrational wave functions  $\mathcal{X}_{3\Delta_1, v2}(R)$ ,  $\mathcal{X}_{1\Sigma^+, v1}(R)$  and electronic-vibrational energies were evaluated on the basis of the 20-electron SODCI calculations.

The ‘‘atomic core’’ properties  $A_{\parallel}$  and  $E_{\text{eff}}$  were calculated only for the  ${}^3\Delta_1$  state at the point 3.4 a.u., which is close to the equilibrium distance (see Table III). Before calculating the core properties the shapes of the four-component molecular spinors are restored in the inner core region after the two-component GRECP calculation of the molecule. For this purpose the nonvariational one-center restoration method [18, 19, 21, 22, 26, 55] is applied. The main contribution to the electric field,  $\mathbf{E}$ , in eq. 2 gives the nuclear charge of Hf. In the present paper the Hf nucleus is modeled by a uniform charge distribution within a sphere with radius  $R_{\text{nucl}} = 6.8\text{fm}$ . Taking into accounting that the electric field from electrons leads to a small correction (about one per cent [56]) and the dominant contribution is going from the inner core electrons, we consider here only direct contributions of electrostatic interaction from the closed shells with  $n = 1 - 4$  with the EDMs of other (valence and outer-core) electrons.

## RESULTS AND DISCUSSION.

The calculated potential energy curves of  $\text{HfF}^+$  are shown in Fig. 1. The potential energy curves are taken from ten-electron calculations but shifted (on the energy axis) to fit the  $D_e$  value obtained in the twenty-electron calculations and  $T_e$  values obtained with twenty-electron correction at point  $R = 3.4\text{a.u.}$  The results of calculations for  $\text{HfF}^+$  spectroscopic parameters are presented in

Table III. The first point to note is that the cation is deeply bound. The second important result is that the  ${}^1\Sigma^+$  state appears to be the ground one and the  ${}^3\Delta_1$  state is the first excited one. In addition, the excitation energy from  ${}^1\Sigma^+$  to  ${}^3\Delta_1$  is increased from 866 to 1633  $\text{cm}^{-1}$  after including the  $5s$  and  $5p$  shells of Hf and  $1s$  shell of F into the relativistic correlation calculation. Excitation energies from  ${}^1\Sigma^+$  to other calculated low-lying states are also increased. Note also that the values obtained in ten-electron calculations for the lowest four states are in a good agreement with the purely 20-electron calculations when just the core correction described above is taken into account. Accounting for correlation and relaxation of the  $4f^{14}$ -shell would also be desirable for better accuracy but it is too time consuming computationally. Though the  $5s$  and  $5p$  electrons are more strongly bound than the  $4f$  electrons ( $5s$  and  $5p$  orbital energies about 2 and 1.2 times higher, respectively) one should rather expect that correlation and relaxation contributions of the  $4f$  electrons will lead to a substantially smaller change of the spectroscopic properties of  $\text{HfF}^+$ . There are several reasons for this: unlike the  $5s, 5p$  shells, the  $4f$  shell is localized in essentially different space region than the  $5d$  and, particularly,  $6s, 6p$  ones (the average radii of the  $5s$  and  $5p$  shells are about twice larger than that of  $4f$ ); the angular-type  $4f-4f$  and  $4f-6s, 6p$  electron correlations are suppressed because there are no ‘‘relatively low-lying’’  $g$ -states, whereas the lower-lying  $4d$ -states are completely occupied. In Table IV the results of the Dirac-Fock calculations for the transition  $5d^1 6s^1 \rightarrow 5d^0 6s^2$  with  $[\text{Xe}]4f^{14}5s^2 5p^6$  and  $[\text{Xe}]4f^{14}$  frozen core are compared to the all-electron results. Two series of Dirac-Fock calculations are performed; in the first one the cores were taken being frozen from the  $5d^1 6s^1$  state, and in the second one they were extracted from the  $5d^0 6s^2$  state. One can see from Table IV that the influence of  $4f$  relaxation is about one order of magnitude smaller than that of  $5s5p$  relaxation. Similar picture is observed when correlations are taken into account. The results of the all-electron Fock space relativistic coupled cluster (RCC) calculations for the transition from the terms of the  $5d^1 6s^1$  configuration to the  $5d^0 6s^2$  configuration are presented in Table V. Three series of RCC calculations are performed; in ten-electron calculation the  $5s, 5p$  shells are correlated, in sixteen-electron calculation the  $4f$  shells are correlated, in twenty four-electron calculation the  $4f, 5s, 5p$  shells are correlated in addition to the  $5d, 6s, 6p$  ones. So difference between the twenty four-electron and sixteen-electron calculations give us the correlation contribution of the  $5s, 5p$  shells, difference between the twenty four-electron and ten-electron calculations give us the contribution of the correlation of the  $4f$  shell. One can see from Table IV that the influence of  $4f$  correlation is about one order of magnitude smaller than that of  $5s5p$  correlation. In the framework of the ‘‘atom-in-a-molecule’’ model, the  $5d^1 6s^1 \rightarrow 5d^0 6s^2$  excitation of the  $\text{Hf}^{2+}$  fragment gives

the leading contribution to the  $^1\Sigma^+ \rightarrow ^3\Delta_1$  transition of  $\text{HfF}^+$ , and therefore we do not expect changes more than  $100 \text{ cm}^{-1}$  in the energy for the above transition when  $4f$  correlation and relaxation are taken into account. So we do not expect that the order of levels will be changed. The data of transition dipole moments from Table I and Table II can be used to study schemes of populating the  $^3\Delta_1$  state.

The SO splittings of the  $^3\Delta$  and  $^3\Pi$  states are mainly due to the SO splitting of the  $5d$  shell of Hf:

$$\mathbf{H}_{l_s}^{\text{so}} = a \cdot (\mathbf{l}_{5d} \cdot \mathbf{s}_{5d}), \quad (10)$$

The atomic Dirac-Fock calculation of  $\text{Hf}^+$  gives  $\varepsilon_{5/2} - \varepsilon_{3/2} = 3173 \text{ cm}^{-1} \Rightarrow a = 1269 \text{ cm}^{-1}$ , where  $\varepsilon_{5/2}$  and  $\varepsilon_{3/2}$  are orbital energies of the  $5d_{5/2}$  and  $5d_{3/2}$  states of  $\text{Hf}^+$ . The SO interaction (10) averaged over the  $^3\Delta$  or  $^3\Pi$  states is reduced to

$$\mathbf{H}_{LS}^{\text{so}} = \mathcal{A} \cdot (\mathbf{L} \cdot \mathbf{S}), \quad (11)$$

where  $\mathcal{A} = 1269/2 = 635 \text{ cm}^{-1}$ , and  $\mathbf{L}$  and  $\mathbf{S}$  are the orbital momentum and spin moment of  $\text{HfF}^+$ . The SO interaction (11) leads to splitting between the components of the  $^3\Delta$  and  $^3\Pi$  states on  $1269$  and  $635 \text{ cm}^{-1}$ , respectively. It is in good agreement with the splitting of the  $^3\Delta$  state calculated in Table III but with the  $^3\Pi$  splitting because of the off-diagonal SO interaction (which is not described by expression (11)) with closely lying  $^1\Delta$  and  $^1\Pi$  states.

The calculated  $A_{\parallel}$  and  $E_{\text{eff}}$  for the  $^3\Delta_1$  state are presented in Table VI. In contrast to  $A_{\parallel}[\text{F}]$ ,  $A_{\parallel}[\text{Hf}]$  and  $E_{\text{eff}}[\text{Hf}]$  are not seriously changed when the outer core electrons are included into the calculation. This behavior of  $A_{\parallel}[\text{F}]$  is explained by the fact that the shells of fluorine in the molecule can be considered with good accuracy as a closed-shell subsystem (thus having  $A_{\parallel}[\text{F}] \approx 0$ ) in the  $^3\Delta$  state, i.e. there is a large compensation of contributions from orbitals with different projections of total electronic momentum to  $A_{\parallel}[\text{F}]$ . Therefore, even a small perturbation (influencing on the shells of F) can seriously change the  $A_{\parallel}[\text{F}]$  value. The calculated  $E_{\text{eff}}$  is large and comparable with the corresponding value for the  $a(1)$  state of the  $\text{PbO}$  molecule [22]. Our  $E_{\text{eff}}$  value has opposite sign than that obtained by Meyer *et al.* [17] in scalar-relativistic calculations and 1.34 times larger by absolute value. In Table VII we are tabulating lifetimes  $\tau_{\text{el}}$  and  $\tau_{\text{vibr}}$  for the lowest vibrational levels of the  $^3\Delta_1$ . It is difficult to obtain this value accurately because of small absolute values of both transition energies and, particularly, of the transition dipole moments between those states, whereas the absolute errors are similar to those for other transitions. Moreover, the transition energy and dipole moment calculated for the considered transition with rather large *relative errors*, are presented in equation (8) as third and second powers, respectively, thus

TABLE I: Ten-electron SODCI calculations of transition dipole moments and molecule-frame electric dipole moments for  $^3\Delta_1$  state calculated with respect to the center of mass. Axis  $z$  is directed from Hf to F. All values in a.u.

R	3.1	3.3	3.4	3.5	3.7	4.0
$D(R)_{^3\Delta_1 \rightarrow ^3\Delta_1}$	-1.15	-1.40	-1.52	-1.64	-1.87	-2.20
$D(R)_{^1\Sigma^+ \rightarrow ^3\Delta_1} \cdot 10^2$	1.60	1.59	1.60	1.56	1.50	1.14
$D(R)_{^1\Sigma^+ \rightarrow ^3\Pi_1} \cdot 10^1$	3.12	2.94	2.84	2.77	2.69	2.70
$D(R)_{^1\Sigma^+ \rightarrow ^1\Pi_1} \cdot 10^1$	7.55	6.52	6.02	5.59	4.93	4.11
$D(R)_{^3\Delta_1 \rightarrow ^3\Pi_1} \cdot 10^2$	3.78	4.00	4.13	4.25	4.51	4.99
$D(R)_{^3\Delta_1 \rightarrow ^1\Pi_1} \cdot 10^2$	3.34	3.90	3.87	3.93	4.09	4.50
$D(R)_{^3\Delta_1 \rightarrow ^3\Pi_{0+}} \cdot 10^1$	3.86	3.30	3.01	2.80	2.45	2.13

seriously increasing the relative error for the lifetimes of  $^3\Delta_1$ . The correction factors  $(D^{10e}(3.4)/D^{20e}(3.4))^2$  calculated from data of Table I and Table II for  $\tau_{\text{el}}$  and  $\tau_{\text{vibr}}$  are 0.673 and 1.028, respectively. Finally, it should be noted that the calculated energy for the  $^1\Sigma^+ \rightarrow ^3\Pi_1$  transition is in a good agreement with the pilot experimental datum by Cornell group [57].

#### ACKNOWLEDGMENTS.

N.M. and A.T. are grateful to RFBR for grant No. 06-03-33060, the partial support from RFBR grant No. 07-03-01139 is also acknowledged. A.P. is also supported by grant of the Governor of Leningrad district. The authors thank E.Cornell for stimulating this work and for many useful discussions.

\* Electronic address: anpetrov@pnpi.spb.ru; Also at St.-Petersburg State University, St.-Petersburg, Russia

† Also at St.-Petersburg State University, St.-Petersburg, Russia

- [1] B. C. Regan, E. D. Commins, C. J. Schmidt, and D. DeMille, *Phys. Rev. Lett.* **88**, 071805 (2002).
- [2] O. P. Sushkov and V. V. Flambaum, *Sov. Phys.-JETP* **48**, 608 (1978).
- [3] V. G. Gorshkov, L. N. Labzovsky, and A. N. Moskalyov, *Sov. Phys.-JETP* **49**, 209 (1979).
- [4] A. V. Titov, N. S. Mosyagin, A. N. Petrov, T. A. Isaev, and D. P. DeMille, *Progr. Theor. Chem. Phys.* **B 15**, 253 (2006).
- [5] B. E. Sauer, H. T. Ashworth, J. J. Hudson, M. R. Tarbutt, and E. A. Hinds, *Atomic Physics* **20**, 44 (2006).
- [6] J. S. M. Ginges and V. V. Flambaum, *Phys. Rep.* **397**, 63 (2004).
- [7] J. Erler and M. J. Ramsey-Musolf, *Prog. Part. Nucl. Phys* **54**, 351 (2005).
- [8] D. Kawall, F. Bay, S. Bickman, Y. Jiang, and D. DeMille, *Phys. Rev. Lett.* **92**, 133007 (2004).
- [9] R. Stutz and E. Cornell, *APS Meeting Abstracts* pp. J1047+ (2004).

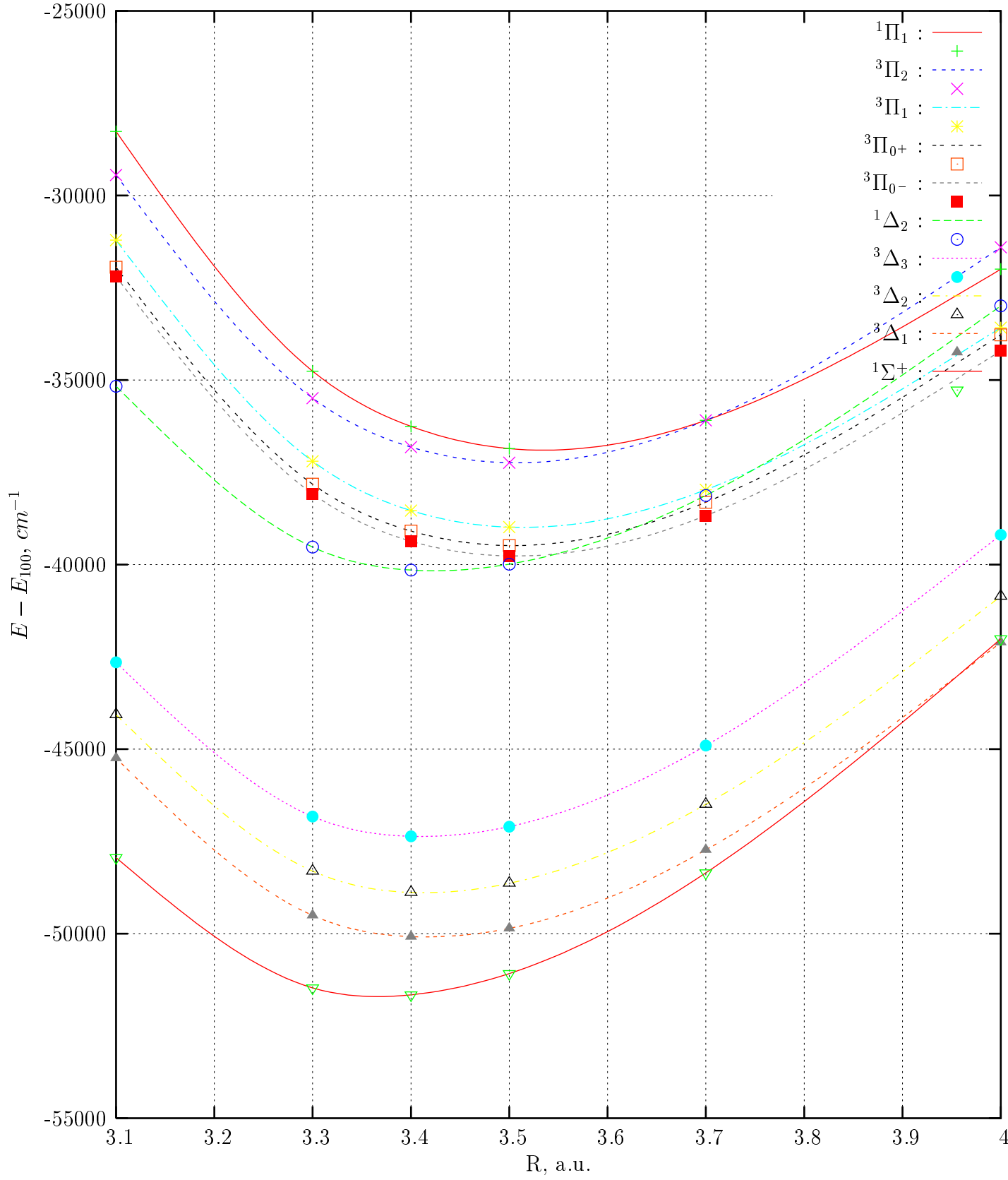




TABLE III: Calculated spectroscopic parameters for  $\text{Hf}^{2+}$ 

State	$R_e \text{ \AA}$	$T_e \text{ cm}^{-1}$	$T_e$ with core correction <sup>a</sup>	$w_e \text{ cm}^{-1}$	$D_e \text{ cm}^{-1}$
<b>10-electron calculation</b>					
$^1\Sigma^+$	1.784	0	0	751	51107
$^3\Delta_1$	1.810	866	1599	718	
$^3\Delta_2$	1.809	1821	2807	719	
$^3\Delta_3$	1.807	3201	4324	721	
$^1\Delta_2$	1.814	9246	11519	696	
$^3\Pi_{0-}$	1.856	9466	11910	689	
$^3\Pi_{0+}$	1.854	9753	12196	699	
$^3\Pi_1$	1.860	10190	12686	687	
$^3\Pi_2$	1.856	11898	14438	703	
$^1\Pi_1$	1.870	12642	14784	679	
<b>20-electron calculation</b>					
$^1\Sigma^+$	1.781	0		790	51685
$^3\Delta_1$	1.806	1633		746	
$^3\Delta_2$	1.805	2828		748	
$^3\Delta_3$	1.804	4273		749	

<sup>a</sup> See section “Methods and calculations” for details.

TABLE IV: Transition energies (in  $\text{cm}^{-1}$ ) for the  $5d^16s^1 \rightarrow 5d^06s^2$  obtained in Dirac-Fock calculations of the  $\text{Hf}^{2+}$  ion.

Frozen core	$[\text{Xe}]4f^{14}5s^25p^6$	$[\text{Xe}]4f^{14}$	all electron included
Frozen from $5d^16s^1$	13 322	12 621	12 439
Frozen from $5d^06s^2$	11 499	12 264	12 439

- [10] B. Ravaine, S. G. Porsev, and A. Derevianko, *Phys. Rev. Lett.* **94**, 013001 (2005).
- [11] T. A. Isaev, N. S. Mosyagin, A. N. Petrov, and A. V. Titov, *Phys. Rev. Lett.* **95**, 163004 (2005).
- [12] L. Sinclair, J. Bohn, A. Leanhardt, P. Maletinsky, E. M. R. Stutz, and E. Cornell, in *36th APS Meeting Abstracts* (APS, Lincoln, Nebraska, 2005), p. 6119.
- [13] E. Cornell and A. Leanhardt (2006), private communication.
- [14] A. N. Petrov, N. S. Mosyagin, T. A. Isaev, and A. V. Titov, *Phys. Rev. A* **75**, 030501(R) (2007).
- [15] M. G. Kozlov, V. I. Fomichev, Yu. Yu. Dmitriev, L. N. Labzovsky, and A. V. Titov, *J. Phys. B* **20**, 4939 (1987).
- [16] M. Kozlov and L. Labzovsky, *J. Phys. B* **28**, 1933 (1995).
- [17] E. R. Meyer, J. L. Bohn, and M. P. Deskevich, *Phys. Rev. A* **73**, 062108 (2006).
- [18] A. V. Titov, Ph.D. thesis, St.-Petersburg (Leningrad) State University, Russia (1985).
- [19] A. V. Titov, *Int. J. Quantum Chem.* **57**, 453 (1996).
- [20] N. S. Mosyagin, M. G. Kozlov, and A. V. Titov, *J. Phys. B* **31**, L763 (1998).
- [21] A. N. Petrov, N. S. Mosyagin, T. A. Isaev, A. V. Titov, V. F. Ezhov, E. Eliav, and U. Kaldor, *Phys. Rev. Lett.* **88**, 073001 (2002).
- [22] A. N. Petrov, A. V. Titov, T. A. Isaev, N. S. Mosyagin, and D. P. DeMille, *Phys. Rev. A* **72**, 022505 (2005).
- [23] Yu. Yu. Dmitriev, Yu. G. Khait, M. G. Kozlov, L. N. Labzovsky, A. O. Mitrushenkov, A. V. Shtoff, and A. V. Titov, *Phys. Lett. A* **167**, 280 (1992).
- [24] G. Theurich and N. A. Hill, *Phys. Rev. B* **64**, 073106, 1 (2001).
- [25] W. C. Ermler, R. B. Ross, and P. A. Christiansen, *Adv. Quantum Chem.* **19**, 139 (1988).
- [26] A. V. Titov and N. S. Mosyagin, *Int. J. Quantum Chem.* **71**, 359 (1999).
- [27] A. V. Titov and N. S. Mosyagin, *Russ. J. Phys. Chem.* **74**, Suppl. 2, S376 (2000), [arXiv: physics/0008160].
- [28] V. Bonifacic and S. Huzinaga, *J. Chem. Phys.* **60**, 2779 (1974).
- [29] A. N. Petrov, N. S. Mosyagin, A. V. Titov, and I. I. Tupitsyn, *J. Phys. B* **37**, 4621 (2004).
- [30] N. S. Mosyagin, A. N. Petrov, A. V. Titov, and I. I. Tupitsyn, in *Recent Advances in the Theory of Chemical and Physical Systems*, edited by J.-P. Julien, J. Maruani, D. Mayou, S. Wilson, and G. Delgado-Barrio (Springer, Dordrecht, The Netherlands, 2006), vol. B 15 of *Progr. Theor. Chem. Phys.*, pp. 229–251.
- [31] N. S. Mosyagin and A. V. Titov, *J. Chem. Phys.* **122**, 234106 (2005).
- [32] A. V. Titov, N. S. Mosyagin, A. N. Petrov, T. A. Isaev, and D. P. DeMille, in *Recent Advances in the Theory of Chemical and Physical Systems*, edited by J.-P. Julien, J. Maruani, D. Mayou, S. Wilson, and G. Delgado-Barrio (Springer, Dordrecht, The Netherlands, 2006), vol. B 15 of *Progr. Theor. Chem. Phys.*, pp. 253–283.
- [33] A. V. Titov, A. O. Mitrushenkov, and I. I. Tupitsyn, *Chem. Phys. Lett.* **185**, 330 (1991).
- [34] N. S. Mosyagin, A. V. Titov, and A. V. Tulub, *Phys. Rev. A* **50**, 2239 (1994).
- [35] A. V. Titov and N. S. Mosyagin, in *Relativistic Effects in Heavy-Element Chemistry (REHE)* (Berlin, Germany, 2003), oral report.
- [36] A. V. Titov, *Doctorate Thesis*, (Petersburg Nuclear Physics Institute, Russian Academy of Sciences, 2002) [in Russian].
- [37] A. V. Titov and N. S. Mosyagin, to be published.
- [38] N. S. Mosyagin and A. V. Titov, arXiv.org/physics/9808006 (1998).
- [39] A. V. Titov and N. S. Mosyagin, arXiv.org/physics/0008239 (2000).
- [40] I. I. Tupitsyn, N. S. Mosyagin, and A. V. Titov, *J. Chem. Phys.* **103**, 6548 (1995).
- [41] N. S. Mosyagin, A. V. Titov, and Z. Latajka, *Int. J. Quantum Chem.* **63**, 1107 (1997).
- [42] A. V. Titov, N. S. Mosyagin, A. B. Alekseyev, and R. J. Buenker, *Int. J. Quantum Chem.* **81**, 409 (2001).
- [43] P. Hafner and W. H. E. Schwarz, *Chem. Phys. Lett.* **65**, 537 (1979).
- [44] A. V. Titov, A. N. Petrov, A. I. Panin, and Y. G. Khait, program package for calculation of molecular matrix elements with the Generalized RECP.
- [45] R. J. Buenker and S. Krebs, in *Recent Advances in Multireference Methods*, edited by K. Hirao (World Scientific, Singapore, 1999), pp. 1–29.
- [46] A. B. Alekseyev, H.-P. Liebermann, and R. J. Buenker, in *Recent Advances in Relativistic Molecular Theory*, edited by K. Hirao and Y. Ishikawa (World Scientific, Singapore,

TABLE V: Transition energies (in  $\text{cm}^{-1}$ ) from the terms of the  $5d^16s^1$  configuration to the  $5d^06s^2$  configuration obtained in RCC calculations of the  $\text{Hf}^{2+}$  ion.

Transition from	ten-electron calculation	sixteen-electron calculation	twenty four-electron calculation	contribution from $5s5p$	contribution from $4f$
$6s_{1/2}5d_{3/2}(J=1)$	9233	10899	9182	-1717	-51
$6s_{1/2}5d_{3/2}(J=2)$	8935	11353	8817	-2536	-118
$6s_{1/2}5d_{5/2}(J=2)$	6251	8763	6036	-2727	-215
$6s_{1/2}5d_{5/2}(J=3)$	5168	6991	4973	-2018	-195

TABLE VI: Calculated parameters  $A_{\parallel}[\text{Hf}]$  and  $A_{\parallel}[\text{F}]$  (in MHz) and  $E_{\text{eff}}$  (in  $10^{24}\text{Hz}/(e \cdot \text{cm})$ ) for the  ${}^3\Delta_1$  state of  ${}^{177}\text{Hf}^{19}\text{F}^+$  at internuclear distance of 3.4 a.u.

$A_{\parallel}[\text{Hf}]$	$A_{\parallel}[\text{F}]$	$E_{\text{eff}}$
<b>10-electron calculation</b>		
-1250	-33.9	5.89
<b>20-electron calculation</b>		
-1239	-58.1	5.84

TABLE VII: Calculated vibrational energy levels (in  $\text{cm}^{-1}$ ) of the  ${}^1\Sigma^+$  and  ${}^3\Delta_1$  states and radiational lifetimes (in seconds) of the  ${}^3\Delta_1$  state.

$v$	${}^1\Sigma^+$		${}^3\Delta_1$	
	$E_v$		$\tau_{\text{el}}$	$\tau_{\text{vibr}}$
0	416	368	0.389	-
1	1234	1117	0.365	0.184
2	2038	1878	0.343	0.088
3	2821	2631	0.316	0.059
4	3586	3373	0.290	0.046

- 2004), pp. 65–105.
- [47] Z. Gershgorin and I. Shavitt, *Int. J. Quantum Chem.* **2**, 751 (1968).
- [48] P. J. Bruna, S. D. Peyerimhoff, and R. J. Buenker, *Chem. Phys. Lett.* **72**, 278 (1980).
- [49] E. R. Davidson, in *The World of Quantum Chemistry*, edited by R. Daudel and B. Pullman (Reidel, Dordrecht, Holland, 1974), pp. 17–30.
- [50] N. S. Mosyagin, A. V. Titov, R. J. Buenker, H.-P. Liebermann, and A. B. Alekseyev, *Int. J. Quantum Chem.* **88**, 681 (2002).
- [51] N. S. Mosyagin, E. Eliav, A. V. Titov, and U. Kaldor, *J. Phys. B* **33**, 667 (2000).
- [52] T. A. Isaev, N. S. Mosyagin, M. G. Kozlov, A. V. Titov, E. Eliav, and U. Kaldor, *J. Phys. B* **33**, 5139 (2000).
- [53] K. Andersson, M. R. A. Blomberg, M. P. Fülscher, G. Karlström, R. Lindh, P.-A. Malmqvist, P. Neogrády, J. Olsen, B. O. Roos, A. J. Sadlej, et al. (1999), quantum-chemical program package “MOLCAS”, Version 4.1.
- [54] J. Olsen and B. O. Roos, *J. Chem. Phys.* **89**, 2185 (1988).
- [55] A. V. Titov, N. S. Mosyagin, and V. F. Ezhov, *Phys. Rev. Lett.* **77**, 5346 (1996).
- [56] E. Lindroth, B. W. Lynn, and P. G. H. Sandars, *J. Phys. B* **22**, 559 (1989).
- [57] E. Cornell et al., to be published.